

# Testing General Relativity with Current Cosmological Data

Scott F. Daniel<sup>1</sup>, Eric V. Linder<sup>1,2,3</sup>, Tristan L. Smith<sup>3</sup>, Robert R. Caldwell<sup>4</sup>, Asantha Cooray<sup>5</sup>, Alexie Leauthaud<sup>2,3</sup>, Lucas Lombriser<sup>6</sup>

<sup>1</sup>*Institute for the Early Universe, Ewha Womans University, Seoul, Korea*

<sup>2</sup>*Lawrence Berkeley National Laboratory, Berkeley, CA, USA*

<sup>3</sup>*Berkeley Center for Cosmological Physics, University of California, Berkeley, CA, USA*

<sup>4</sup>*Department of Physics and Astronomy, Dartmouth College, Hanover, NH, USA*

<sup>5</sup>*Department of Physics and Astronomy, University of California, Irvine, CA, USA*

<sup>6</sup>*Institute for Theoretical Physics, University of Zürich, Switzerland*

(Dated: October 23, 2018)

Deviations from general relativity, such as could be responsible for the cosmic acceleration, would influence the growth of large scale structure and the deflection of light by that structure. We clarify the relations between several different model independent approaches to deviations from general relativity appearing in the literature, devising a translation table. We examine current constraints on such deviations, using weak gravitational lensing data of the CFHTLS and COSMOS surveys, cosmic microwave background radiation data of WMAP5, and supernova distance data of Union2. A Markov Chain Monte Carlo likelihood analysis of the parameters over various redshift ranges yields consistency with general relativity at the 95% confidence level.

## I. INTRODUCTION

The nature of gravitation across cosmological ages and distances remains a frontier of current knowledge as we try to understand the origin of the cosmic acceleration [1, 2]. Newly refined observations of cosmic structure [3, 4] make it possible to test the predictions of general relativity (GR) for its influence on the growth of cosmic structure through gravitational instability and the gravitational lensing deflection of light by that structure. Indications of a deviation from GR would have profound consequences for cosmology, as well as for fundamental physics.

To explore for new gravitational phenomena, it is useful to parameterize the deviations from GR in the gravitational field equations. A common approach is to introduce two new parameters. The first parameter imposes a relation between the two gravitational potentials entering Newton’s gravitational law of acceleration and the Poisson equation. These are equal in GR in the absence of anisotropic stress but different in many theories of modified gravity. The second parameter establishes a new relation between the metric and matter through a modified Poisson-Newton equation, which can be viewed as turning Newton’s gravitational constant into an effective function of time and space. Numerous realizations of these relations have been put forward in the literature [5–18].

One motivation for our study is to attempt to relate these disparate, but closely related, approaches. Furthermore, many studies have focused on the ability of future measurements to discriminate among various models and to carry out parameter estimation [19–30], however there is sufficient data at present to evaluate preliminary tests of GR [31–34, 36–38]. We concentrate here on current constraints, which also allows us to examine a recent claim of a possible departure from GR [39].

The main points of this article are thus to 1) clar-

ify the relation between different parameterizations and what the degrees of freedom are in a consistent system of equations of motion, 2) confront the parameters encoding deviations from GR with current data to test the theory of gravity, and 3) discuss which features of the data have the most sensitivity to such a test and what astrophysical systematics may most easily mimic a deviation.

In Sec. II we lay out the gravitational field equations in terms of the metric potentials and matter perturbations and compare several forms of parameterizations, giving a “translation table” between them. We illustrate in Sec. III the influence of the parameters on the cosmic microwave background (CMB) temperature power spectrum, the matter growth and power spectrum, and the weak lensing shear statistics. Using Markov Chain Monte Carlo (MCMC) techniques, we then constrain the deviation parameters with current data in Sec. IV. We briefly discuss astrophysical systematics and future prospects in Sec. V.

## II. SYSTEMS OF PARAMETERIZING GRAVITY

The most accurate observations of the effects of gravity have been made in the local universe, e.g. within the solar system and in binary neutron star systems [40–43]. These observations can be used to distinguish between various theories of gravity through the parameterized post-Newtonian (PPN) formalism [44, 45]. The standard PPN formalism introduces a set of constant parameters that take on various values in different gravity theories. This, however, does not give a full description of possible deviations from General Relativity over cosmological scales.

Recent interest in modified gravity has concentrated on those theories that can serve as an alternative explanation for the current period of accelerated cosmic ex-

pansion. In order for modifications producing late-time acceleration on cosmic scales to agree with local tests of gravity they must contain length and/or time dependent modifications, which do not occur in the standard PPN formalism. Moreover, for some theories the natural arena for the PPN formalism – solar system and binary neutron star system observations – may be less discriminating than cosmological tests of gravity, given that the modifications are on large scales. This has led to efforts to establish a parameterized formalism that allows for meaningful comparison between modified gravity theories within a cosmological framework [5–18], without assuming a specific model.

### A. Degrees of Freedom

Changes in the laws of gravitation affect the relationship between the metric and matter variables. Let us explore the degrees of freedom available to define this relation. Restricting our attention to scalar degrees of freedom of the gravitational field, the metric has only two physically relevant scalar functions, or potentials, given by the line element (in conformal-Newtonian gauge, adopting the notation of [46])

$$ds^2 = a^2 [-(1 + 2\psi) d\tau^2 + (1 - 2\phi) d\vec{x}^2], \quad (1)$$

where  $a$  is the scale factor,  $\tau$  the conformal time, and  $x$  the spatial coordinate. In addition to the metric potentials  $\phi$  and  $\psi$ , perturbations to a perfect fluid introduce four additional scalar functions: density perturbations  $\delta\rho$ , pressure perturbations  $\delta p$ , velocity (divergence) perturbations  $\theta$ , and a possible nonzero anisotropic stress  $\sigma$ .

The dynamics of any particular theory are then specified when six independent relations between these six quantities are given. Further restricting attention to those gravity theories that maintain the conservation of stress energy,  $\nabla^\mu T_{\mu\nu} = 0$ , the resulting generalized continuity and Euler equations give two scalar equations and the gravitational field equations supply the remaining four [46].

Since the cosmic expansion shifted from deceleration to acceleration only recently, since  $z < 0.5$  [47], gravity theories that account for this transition without any physical dark energy require a significant departure from GR at late times. Consequently, nonrelativistic matter is the dominant component of the cosmological fluid and so  $\delta p = \delta p_m = 0$  and  $\sigma = \sigma_m = 0$ . Hence, in these theories the dynamically important equations consist of two, as yet unspecified gravitational field equations and the two equations of stress-energy conservation applied to matter, which in Fourier-space are given by

$$\dot{\delta}_m = -\theta_m + 3\dot{\phi}, \quad (2)$$

$$\dot{\theta}_m = -\mathcal{H}\theta_m + k^2\psi. \quad (3)$$

In the above equations,  $\delta_m \equiv \delta\rho_m/\bar{\rho}_m$  with  $\bar{\rho}_m$  the homogeneous part of the matter density,  $\mathcal{H} \equiv \dot{a}/a$ , the dot

denotes a derivative with respect to conformal time, and  $k$  is the wavenumber. There still remains freedom in setting the two gravitational field equations to close the system, subject to the requirement that the theory approaches GR within the solar system.

The two field equations that can close the system in the case of GR are

$$\nabla^2\phi = 4\pi G a^2 \bar{\rho}_m \Delta_m, \quad (4)$$

$$\psi = \phi, \quad (5)$$

where

$$\Delta_m \equiv \delta_m + \frac{3\mathcal{H}}{k^2}\theta_m. \quad (6)$$

In a wide variety of alternative theories of gravitation, additional scalar degrees of freedom modify the strength of Newton's constant, and enforce a new relationship between the potentials  $\phi$  and  $\psi$ . Therefore, one choice for the modified field equations in Fourier-space is

$$-k^2 \frac{A\phi + B\psi}{A + B} = 4\pi G \mu(\tau, k) \bar{\rho}_m \Delta_m, \quad (7)$$

$$\phi = \eta(\tau, k)\psi, \quad (8)$$

where  $A$  and  $B$  are constants, and  $\mu$  and  $\eta$  are functions of time and scale, which are still to be determined. As we will see, there are many other choices that can be made for the exact form of parameterization. These choices influence the constraints and the correlations between those constraints that particular observations give for a particular set of post-GR parameters. We discuss some of the frameworks in the next subsections.

### B. $\varpi\mu$ CDM

We refer to the equations of motion used in [6, 23, 34, 37] as  $\varpi$ CDM. In  $\varpi$ CDM, the equations of motion for cosmic perturbations are determined by enforcing the relation

$$\psi = [1 + \varpi(\tau, k)]\phi \quad (9)$$

for the potentials arising from non-relativistic matter, where the departure from GR is controlled by the parameter  $\varpi$ . In practice, this is carried out by adding a source to the off-diagonal space-space Einstein equation in order to simulate a smooth transition from GR to modified gravity.

Next, requiring that the new gravitational phenomena do not introduce a preferred reference frame distinguished by a momentum flow, e.g. a  $\theta$  that would be attributed to a dark fluid, the time-space Einstein equation is preserved, whereby

$$-k^2 (\dot{\phi} + \mathcal{H}\psi) = -4\pi G a^2 (\bar{\rho} + \bar{p})\theta. \quad (10)$$

As discussed in [37], preserving the time-space Einstein equation along with the modification in Eq. (9) still results in a correction to the GR Poisson equation. This can be thought of as a consequence of the conservation of stress-energy and the related Bianchi identity as applied to the modified gravitational field equations.

We now propose to extend the  $\varpi$ CDM model, to incorporate a new parameter  $\mu$  that controls the modification to the Poisson equation, i.e.

$$-k^2\phi = \mu(\tau, k) 4\pi G a^2 \bar{\rho}_m \Delta_m. \quad (11)$$

Procedurally, this equation replaces Eq. (10) for obtaining the evolution of the gravitational fields. We call this new parameterization  $\varpi\mu$ CDM and note that in this parameterization the time-space Einstein equation is generally modified, as opposed to in the  $\varpi$ CDM parameterization. Note that setting  $\mu = 1$  does not reproduce the original  $\varpi$ CDM model since there  $\varpi$  itself modifies the Poisson equation as discussed above. This parametrization is consistent with the conservation of large-scale curvature perturbations following an argument made in Ref. [21]. They argue that super-horizon curvature perturbations are conserved, so long as the velocity perturbation  $\theta$  is of order  $(k/\mathcal{H})^2$ . This can be seen to be true from Eq. (A3) presented in the appendix of this work.

### C. PPF Linear Theory

A parameterized post-Friedmann (PPF) framework of linear fluctuations was introduced by [9, 13] to describe modified gravity models that yield cosmic acceleration without dark energy. It captures modifications of gravity on horizon, sub-horizon, and non-linear scales. Once the expansion history is fixed, the model is defined by three functions and one parameter, from which the dynamics are derived by conservation of energy and momentum and the Bianchi identities. Modifications to the relationship between the two metric perturbations are quantified by the metric ratio

$$g(a, k) \equiv \frac{\phi - \psi}{\phi + \psi}. \quad (12)$$

In the linearized Newtonian regime, a second function  $f_G(a)$  relates matter to metric perturbations via

$$-k^2(\phi + \psi) = \frac{8\pi G}{1 + f_G} a^2 \bar{\rho}_m \Delta_m. \quad (13)$$

The corresponding quantity that defines this relationship on superhorizon scales is  $f_\zeta(a)$ . The last quantity that needs to be defined is  $c_\Gamma$ , which determines the transition scale from superhorizon to quasistatic behavior in the dynamical equations (see [9, 13] for details).

The PPF parameters can be directly related to the

$\varpi\mu$ CDM parameters as follows:

$$g = -\frac{\varpi}{2 + \varpi} \quad ; \quad \varpi = -\frac{2g}{1 + g} \quad (14)$$

$$f_G = \frac{2}{\mu(2 + \varpi)} - 1 \quad ; \quad \mu = \frac{1 + g}{1 + f_G}. \quad (15)$$

### D. Gravitational Growth Index $\gamma_G$

Another way to close the system of equations is to specify the evolution of one of the perturbed fluid or metric variables. A standard choice is to determine a specific evolution for  $\Delta_m$  through the gravitational growth index  $\gamma_G$  introduced to parameterize deviations from general relativity in growth by [48]. This was partly tied to the metric potentials in [49] but here we present a more complete relation.

From Eq. (23) of [49] we see the key quantity is the modification of the source term in the Poisson equation, there called  $Q$ . The second order equation for the evolution of the density perturbation arises from  $\nabla^2\psi$ , and there is also a modification  $\mu$  allowed in the gravitational coupling as in Eq. (11). In essence,  $\nabla^2\psi \rightarrow -k^2(1 + \varpi)\phi \rightarrow (1 + \varpi)\mu \times 4\pi G a^2 \bar{\rho}_m \Delta_m$ . Thus  $Q = (1 + \varpi)\mu$ . The relationship between  $\varpi$ ,  $\mu$  and the evolution of  $\Delta_m$  is presented rigorously here in Eq. (A5) (also see Sec. III B).

The gravitational growth index in Eq. (23) of [49] thus relates to the  $\varpi\mu$ CDM formalism through

$$\gamma_G = \frac{3(1 - w_\infty - [(1 + \varpi)\mu - 1]/[1 - \Omega_m(a)])}{5 - 6w_\infty} \quad (16)$$

$$\rightarrow \frac{6}{11} \left( 1 - \frac{\varpi_0 + \mu_0}{2} \frac{\Omega_m}{1 - \Omega_m} \right). \quad (17)$$

Note  $w_\infty$  is an effective high redshift equation of state defined in terms of how the matter density in units of the critical density,  $\Omega_m(a)$ , deviates from unity (specifically,  $w_\infty = [d \ln \Omega_m(a)/d \ln a]/[3(1 - \Omega_m(a))]$ ). In the last line of Eq. (17) we specialize to a  $\Lambda$ CDM expansion history, as used throughout this article, so  $w_\infty = -1$ , and to the ansatz for  $\varpi$  and  $\mu$  used later in Eqs. (18).

### E. Relating Parameterizations

The discussion above is by no means an exhaustive list of the parameterizations proposed in the literature to describe departures from GR. Many more exist, and while all of them have in common a relatively simple parameterization of the departure from  $\phi = \psi$ , they all differ in how they close the system of equations. Some, like  $\varpi\mu$ CDM, modify the Poisson equation directly. Others, like  $\varpi$ CDM, retain one of the Einstein equations.

Table I lists some of the most common parameterizations and presents a useful translation between their post-GR parameters and  $\varpi\mu$ CDM. With the possible

exception of the parameterization from [39] (see next paragraph and its footnote), all of the parameterizations presented are presumed to leave the equations of stress-energy conservation unmodified.

Since none of these model-independent approaches start from an action, one must be careful to trace the system of equations to make sure that the phenomenological modifications do not under- or over-specify the system<sup>1</sup> and do satisfy stress-energy conservation. Another approach involves testing consistency relations valid in GR between observables; see for example [7, 22, 50].

### III. INFLUENCE OF GRAVITY MODIFICATIONS ON OBSERVATIONS

The behavior of the CMB, weak lensing, and matter power spectrum in the  $\varpi$ CDM scenario have been discussed in [34, 37]. The consequences are slightly different when we introduce  $\mu$  in the  $\varpi\mu$ CDM parameterization. In the case that  $\varpi < 0$  and  $\mu < 1$ , both lead to an amplification of low- $\ell$  CMB power;  $\varpi > 0$  and  $\mu > 1$  both suppress it. This allows us to play the two parameters against each other, combining positive (negative) values of  $\varpi$  with smaller (larger) values of  $\mu$  to generate non-GR power spectra that appear to be in better agreement with the data than those obtained within the confines of the  $\varpi$ CDM model. That either parameter can enhance or suppress power results in a degeneracy between  $\varpi$  and  $\mu$  in any multi-parameter exploration of the data. Observations that can break this degeneracy therefore become vital to diagnosing departures from GR.

For the purposes of the discussion in this section, we will assume the redshift dependences

$$\begin{aligned}\varpi &= \varpi_0 a^3 \\ \mu &= 1 + \mu_0 a^3.\end{aligned}\quad (18)$$

Note this form can be motivated by the scaling argument in [49], that the deviations in the expansion history should keep pace with the deviations in the growth history. Otherwise one tends to either violate GR at early times (causing difficulties for primordial nucleosynthesis and the CMB) or does not achieve acceleration by the present. In addition to the CMB, we also discuss the effects of our post-GR parameters on the matter power spectrum and on weak lensing statistics.

<sup>1</sup> A careful reading of [39] reveals that there four unknowns –  $\phi$ ,  $\psi$ ,  $\delta$ , and  $\theta$  – are evolved with five equations – the continuity equation (2), Euler equation (3), Poisson equation (4), and the post-GR parameter equations  $\dot{\phi} = \eta\psi$  and  $\dot{\Delta}_m = \mathcal{H}\Delta_m\Omega_m^{\gamma_G}$ . Thus, the system is over-specified.

#### A. CMB Anisotropy Spectrum

We modified versions of the public Boltzmann codes CMBfast [51] and CAMB [52] to evolve the cosmological perturbations according to parameterization (18) and the equations of motion presented in Sec. II B. We used these codes to generate examples of CMB anisotropy and matter power spectra for different values of  $\varpi_0$  and  $\mu_0$ ; in order to focus on the non-GR effects, in this section all other cosmological parameters are set to their WMAP5 maximum likelihood values [53]. Figure 1 shows the resulting CMB anisotropy spectra. As in [34] for  $\varpi$ CDM, negative values and extreme positive values of the post-GR parameters amplify the power in the low- $\ell$  multipoles. Moderate positive values suppress the low- $\ell$  power. This is a manifestation of the integrated Sachs-Wolfe (ISW) effect. The high- $\ell$  power is unaffected.

The ISW effect arises when time evolving  $\phi$  and  $\psi$  potentials cause a net energy shift in CMB photons. The CMB ISW power is sourced as

$$C_l \sim (\dot{\phi} + \dot{\psi})^2. \quad (19)$$

As was discussed in [37], the evolution of  $\phi$  and  $\psi$  potentials in the universe is a competition between gravitational collapse trying to deepen the potentials and cosmic expansion trying to dilute them. Under GR with a cosmological constant, the expansion wins and the source term for the ISW  $\dot{\phi} + \dot{\psi} > 0$  (note  $\phi, \psi < 0$ ). By weakening gravity,  $\varpi_0$  or  $\mu_0 < 0$  tilts the competition even more towards cosmic expansion, hastening the dilution of  $\phi$  and  $\psi$ , causing  $\dot{\phi} + \dot{\psi}$  to be even larger, and amplifying the ISW effect. Positive  $\varpi_0$  or  $\mu_0$  amplifies gravity – either by directly deepening the Newtonian potential  $\psi$  so that mass is more attractive ( $\varpi_0 > 0$  case) or by causing  $\Delta_m$  to source a deeper potential through the modified Poisson equation ( $\mu_0 > 0$  case) – so that the dilution due to cosmic expansion is slowed, leading to a weaker ISW effect. In the case of extremely positive  $\varpi_0$  or  $\mu_0$  the ISW deepening is so pronounced that the sign of  $\dot{\phi} + \dot{\psi}$  is reversed, but since the ISW effect in the power spectrum depends on the square, the ISW effect is again amplified. High- $\ell$  power is unaffected because the ISW is a sub-dominant effect on those scales.

Figure 2 more clearly illustrates this bimodal behavior by plotting the change in quadrupole power relative to GR as a function of the post-GR parameter, varying one at a time (compare Fig. 4 in [37]). The blue, dot-dashed curve is generated by varying  $\varpi_0$  and holding fixed  $\mu_0 = 0$ . The red, dashed curve is generated by varying  $\mu_0$  and holding fixed  $\varpi_0 = 0$ . Note that the CMB appears to be more sensitive to differing values of  $\mu_0$  than of  $\varpi_0$ . The black, solid curve is generated by varying  $\varpi_0$  and compensating for this by setting  $\mu_0 = 2/(2 + \varpi_0) - 1$ . This choice is motivated by the alternative definition of the unmodified Poisson equation

$$-k^2(\phi + \psi)/2 = 4\pi G a^2 \bar{\rho}_m \Delta_m \quad (20)$$



| parameterization                  | parameter relating $\phi$ and $\psi$                               | closing parameter   | comments   |
|-----------------------------------|--|---|--|
| $\varpi$ CDM [6, 34, 37]          | $\varpi$   | Retains equation (10)   |  |
| Curvature [12]                    | $\gamma_{BZ} = \frac{1}{1+\varpi}$                                 | Conserves curvature perturbations $\zeta$   | Effectively retains Eq. (10).<br>See appendix in Ref. [34]                 |
| PPF [9, 13]                       | $g = -\frac{\varpi}{2+\varpi}$                                     | $f_G = \frac{2}{\mu(2+\varpi)} - 1$   | Includes scale-dependent transition between super- and sub-horizon regimes |
| MGCAMB [20, 21]<br>cf. [7, 8, 10] | $\gamma_{MGC} = \frac{1}{1+\varpi}$<br>$\eta = \frac{1}{1+\varpi}$ | $\mu_{MGC} = \mu(1+\varpi)$<br>$\tilde{G}_{\text{eff}} = \frac{\mu(2+\varpi)}{2}$                     | Modifies Poisson equation with $\psi$ instead of $\phi$ in Eq. (11)        |
| Sub-horizon [10]                  | $\frac{B}{\Gamma_\phi} = 1 + \varpi$                               | $\Gamma_\phi = \mu$   |  |
| Growth index [48]                 | additional   | $\gamma_G = \frac{6}{11} \left( 1 - \frac{\varpi_0 + \mu_0}{2} \frac{\Omega_m}{1 - \Omega_m} \right)$ | Only defines $(\varpi, \mu) \rightarrow \gamma_G$ not inverse              |
| Decoupled [39]                    | $\eta = \frac{1}{1+\varpi}$  | $\gamma_G = \frac{\ln(\Delta_m/\mathcal{H}\Delta_m)}{\ln \Omega_m(a)}$                                | Over-specified (also enforces Poisson eqn).                                |

TABLE I: Translation between several different parameterizations of modified gravity and the  $\varpi\mu$ CDM framework.

(see further discussion in the next section). We see that, for a wide range of values of  $\varpi_0$ , complementary ( $\varpi_0 > 0$  and  $\mu_0 < 0$  or vice-versa) values of  $\mu_0$  cancel out much of the late-time ISW effect found in Fig. 1, as alluded to in the introduction to this section.

### B. Matter Power Spectrum and Weak Lensing Statistics

We investigate the power spectrum of the matter perturbations  $\delta_m$  as a function of wavenumber  $k$  in Fig. 3 for the same set of models. Again the most dramatic post-GR effects occur at large scales. This is not due to any scale dependence in the modifications (we took  $\varpi$  and  $\mu$  to be independent of  $k$ ), but simply from the  $k^2$  factor in the modified Poisson equation (11).

For the weak lensing shear correlation function, as for many other observables, we need to know how overdensities grow with scale factor. In the case of GR and  $\varpi$ CDM, this is a relatively simple proposition since the growth of overdensities  $\Delta_m$  is scale-independent after decoupling. As just discussed, this no longer holds for  $\varpi\mu$ CDM. It is possible, using energy conservation and Eqs. (9) and (11), to derive a second-order differential equation for the evolution of  $\Delta_m$ . We show the derivation and result in the Appendix, and focus here on the parameter dependence.

With the exception of one term on the middle line of Eq. (A5), all of the terms containing metric potential modifications to general relativity (the  $\mu$  and  $\varpi$  terms) are multiplied by a factor of  $\mathcal{H}^2/k^2$ . Hence, we expect that the strongest departures from GR predictions occur for small values of  $k$ . Since the most important aspect for comparing modifications against observations is

the change in shape of the power spectrum, rather than its normalization, in Figure 3 we normalize the power spectrum to agree with  $P_{GR}$  at large  $k$ . The strongest deviation in shape indeed occurs for  $k \lesssim 0.002 \text{ Mpc}^{-1}$ . The one exceptional term in Eq. (A5) is precisely the  $(1+\varpi)\mu$  term discussed in Sec. IID entering the gravitational growth index  $\gamma_G$  formalism, and this will dominate for large values of  $k$ , giving a scale-independent enhancement (suppression) for positive (negative)  $\varpi_0$  or  $\mu_0$ .

Figure 4 plots  $\xi_E$ , the E mode of the weak lensing shear two-point correlation function (Eq. (8) of Ref. [4]), normalized to the value under GR as a function of angular separation on the sky. For the angular scales of interest, the effects of changing  $\mu_0$  and  $\varpi_0$  principally manifest themselves as a renormalization of  $\xi_E$ . This is because the scales plotted are much smaller than the scales ( $k \sim \mathcal{H}$ ) at which shape-changing effects manifested themselves in Figure 3. Non-linear power is treated using the usual subroutine halofit based on the semi-analytic fitting scheme presented in Ref. [35]. While we acknowledge that this is not strictly appropriate for modified gravity, we have no reason to think that the effect will be substantial for reasonable values of  $\mu_0$  and  $\varpi_0$ . Furthermore, the constraints presented below in Section IV appear to principally derive from effects at the low- $k$ , rather than the high- $k$ , limit.

## IV. CONSTRAINTS ON DEVIATIONS FROM GR

We now examine constraints imposed by current data on deviations from GR, allowing a large set of cosmological parameters to vary simultaneously. The investi-

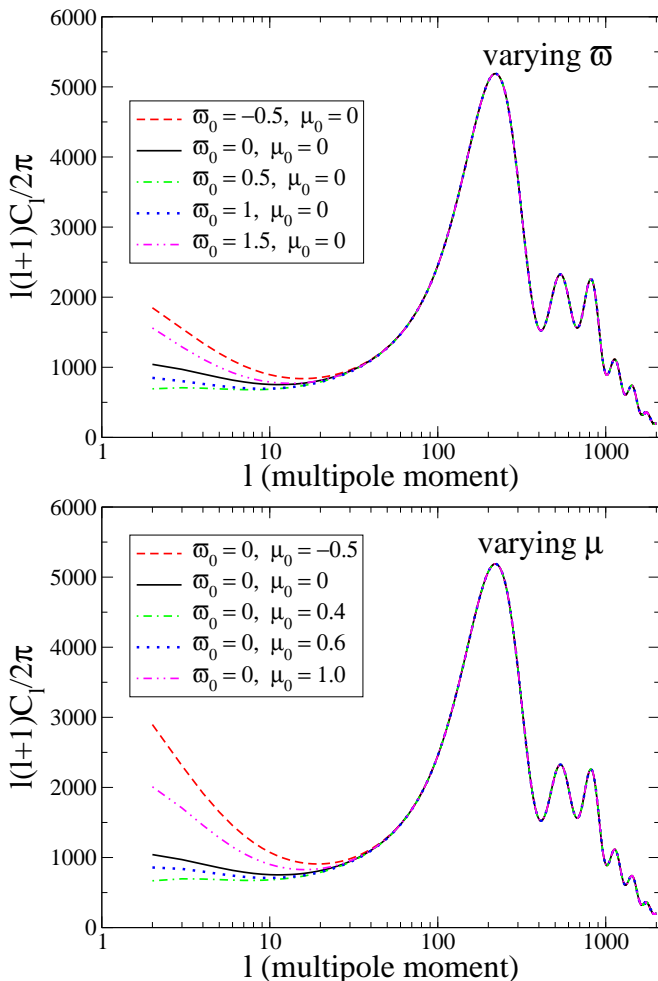


FIG. 1: CMB anisotropy spectra are plotted as a function of the parameters  $\varpi_0$  and  $\mu_0$  in Eqs. (18). As in [34], the post-GR effects all occur in the low- $l$  multipoles. The CMB anisotropy is more sensitive to variations in  $\mu_0$  than to variations in  $\varpi_0$ . See Fig. 2 for more on this point and on varying  $\varpi_0$  and  $\mu_0$  simultaneously.

gation includes two different functional dependences for the gravitational modification parameters  $\varpi(a)$  and  $\mu(a)$ . The first model for the post-GR parameter form does not assume a particular redshift dependence but allows  $\varpi$  and  $\mu$  to take independent values in each of three redshift bins. (In fact, we slightly smooth the transitions so as to avoid infinities in the derivatives entering the ISW effect, with a transition modeled by an arctan form of width  $\Delta a = 0.01$ .) That is,  $\mu = \{1 + \mu_{0a}, 1 + \mu_{0b}, 1 + \mu_{0c}\}$  and  $\varpi = \{\varpi_{0a}, \varpi_{0b}, \varpi_{0c}\}$  for  $\{2 < z \leq 9, 1 < z \leq 2, z \leq 1\}$ . We assume that  $\varpi$  and  $\mu$  are scale-independent. For  $z > 9$  we assume that differences from GR are negligible so  $\mu = 1$  and  $\varpi = 0$ .

We test this theory against the data using a modified version of the public MCMC code COSMOMC [52, 54, 55] with a module (first presented in [56]) to incorporate the COSMOS weak lensing tomography data

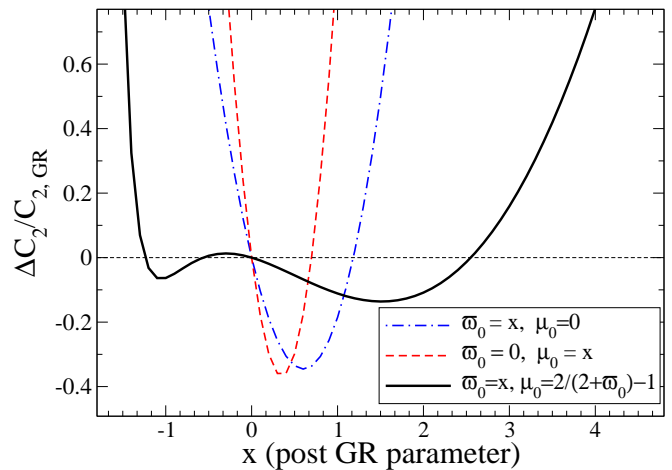


FIG. 2: The change in quadrupole power relative to the value in GR is plotted as a function of  $\varpi_0$  and  $\mu_0$ . The blue, dot-dashed curve shows the effects of varying  $\varpi_0$  with fixed  $\mu_0 = 0$ . The red, dashed curve shows the effects of varying  $\mu_0$  with fixed  $\varpi_0 = 0$ . One can mimic the unmodified GR CMB spectrum over a much wider range of post-GR parameter values by simultaneously varying  $\varpi_0$  and  $\mu_0$  in opposite directions, as shown in the black, solid curve using  $\mu_0 = 2/(2 + \varpi_0) - 1$ . The horizontal dotted line denotes perfect agreement with GR.

[3] and data from the CFHTLS survey [4]. We also include WMAP5 CMB data [57–59] and Union2 supernova distance data [60]. In all cases, we use the full covariance matrix (including systematics in the Union2 case) provided by the group who collected and initially analyzed the data. In addition to the post-GR parameters, the parameter set includes  $\Omega_b h^2$ ,  $\Omega_c h^2$ ,  $\theta$  (the ratio of the sound horizon to the angular diameter distance to last scattering),  $\tau$  (the optical depth to reionization),  $n_s$ , the amplitude of the SZ effect, and the amplitude of primordial scalar perturbations. We assume that  $w = -1$  for our effective dark energy, that  $\Omega_K = 0$ , and that there are no massive neutrinos contributing to dark matter. Each weak lensing data set requires 3 nuisance parameters. Thus, we integrate over a total of up to 16 parameters, depending on the data sets used and the parametrization of  $\mu$  and  $\varpi$  chosen. Under the binned parametrization, we vary  $\mu$  or  $\varpi$  but not both simultaneously, which would require 19 independent parameters. This choice was made both for convenience and to reproduce the analysis of Ref. [39]. Additional MCMC calculations done in which both  $\mu$  and  $\varpi$  were allowed to vary in all three bins also returned results consistent with GR in the presence of a cosmological constant.

Figure 5 shows the marginalized probabilities on the  $\varpi_{0a,b,c}$  parameters for runs in which  $\mu_{0a,b,c} = 0$ , so that  $\mu = 1$  and the Poisson equation defined as in Eq. (4) remains valid at all redshifts. Figure 6 shows similar constraints on  $\mu_{0a,b,c}$  in the case where  $\varpi_{0a,b,c} = 0$ . Our results in all cases are consistent with GR within the 95% confidence limit, although they do allow the possibility

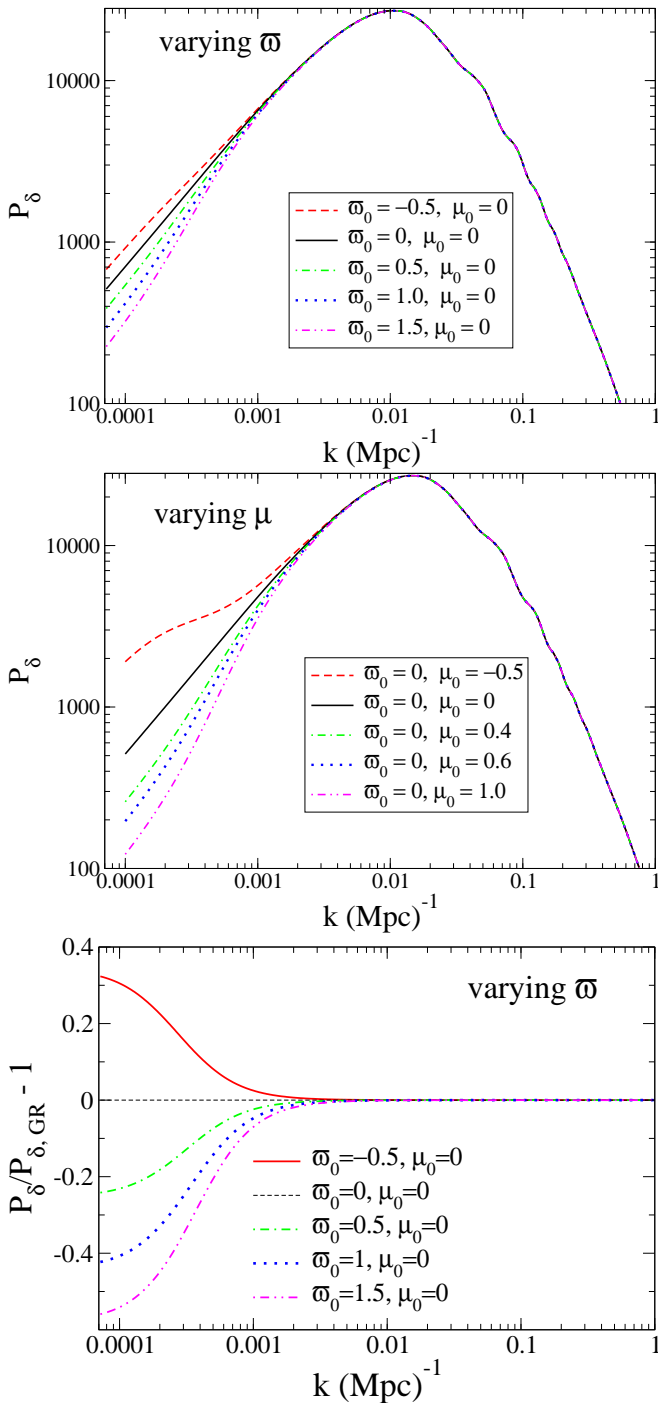


FIG. 3: We plot the matter power spectrum (normalized to  $k = 1 \text{ Mpc}^{-1}$ ) generated by varying the parameters  $\varpi_0$  and  $\mu_0$ . Unlike under  $\varpi\text{CDM}$  [34], even our scale-independent parameterization has scale-dependent effects due to the  $k^2$  factor in the Poisson equation. The bottom panel shows the residuals of the top panel, i.e. the deviation relative to GR when varying  $\varpi_0$  (the  $\mu_0$  case looks similar), to highlight the scale-dependent regime at low  $k$  and scale-independent regime at high  $k$ .

of departures from GR with  $\varpi_0$  or  $\mu_0 \sim 0.1$ .

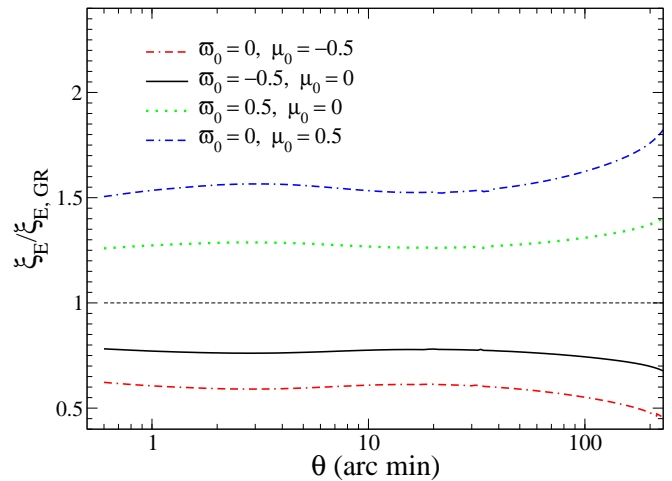


FIG. 4: We plot the ratio of the E mode of the weak lensing shear two-point correlation function (Eq. 8 of [4]) to the same statistic calculated in GR, with all parameters but either  $\varpi_0$  or  $\mu_0$  fixed, to see the influence of the non-GR parameters. For the most part, post-GR parameters serve to renormalize the correlation function. As with the CMB anisotropy and matter power spectra, the effect is more sensitive to changes in  $\mu_0$  than to changes in  $\varpi_0$ .

Constraints on the usual cosmological parameters are largely unaffected by the introduction of  $\mu$  and  $\varpi$ . Mean values shift by less than  $\sim 1\sigma$  and marginalized uncertainties are comparable between GR and non-GR MCMC runs. The only notable exceptions are  $\sigma_8$  and  $\Omega_c h^2$  (the physical density of cold dark matter in the universe), whose marginalized uncertainties increase by up to a factor 2.3 upon the introduction of post-GR parameters. This is consistent with the observation that  $\mu$  and  $\varpi$  principally modify the growth history of cosmological perturbations.

Figure 7 plots the 2-dimensional confidence contours for the post-GR parameters  $\varpi_0, \mu_0$  in the case of redshift dependence as in Eqs. (18). Note that since this parameterization has the strongest effect at low redshift, the greater sky area of CFHTLS has more leverage in constraining the parameters than the greater depth of COSMOS. For the binned parametrization, the constraints from MCMC runs with WMAP5+Union2+CFHTLS (no COSMOS) were indistinguishable from those including COSMOS as well, supporting the supposition that the sky coverage of CFHTLS is, for current data, more important than the redshift depth of COSMOS in constraining the post-GR parameters.

Table II presents the 95% constraints on our post-GR parameters for all of the MCMC calculations considered in Figures 5-7. All of the results are consistent with GR.

We also note that in Figure 7 the contours exhibit the same degeneracy implied by Figure 2. Apparently, the probe of growth provided by current weak lensing data is not able to add much more leverage to the CMB data. This can also be seen in the lack of significant change

| Binned $\varpi$ , $\mu = 1$ : |                               | Binned $\mu$ , $\varpi = 0$ : |                         | Parameterization (18):  |  |
|-------------------------------|-------------------------------|-------------------------------|-------------------------|-------------------------|--|
| COSMOS                        | +CFHTLS                       | +CFHTLS                       | COSMOS                  | +CFHTLS                 |  |
| $-0.11 < \varpi_{0a} < 0.12$  | $-0.15 < \varpi_{0a} < 0.060$ | $-0.074 < \mu_{0a} < 0.080$   | $-1.4 < \varpi_0 < 2.8$ | $-1.6 < \varpi_0 < 2.7$ |  |
| $-0.098 < \varpi_{0b} < 0.23$ | $-0.13 < \varpi_{0b} < 0.18$  | $-0.058 < \mu_{0b} < 0.14$    | $-0.67 < \mu_0 < 2.0$   | $-0.83 < \mu_0 < 2.1$   |  |
| $-0.054 < \varpi_{0c} < 0.39$ | $-0.074 < \varpi_{0c} < 0.33$ | $-0.023 < \mu_{0c} < 0.22$    |                         |                         |  |

TABLE II: 95% confidence limits on post-GR parameters in the MCMC calculations considered in Figures 5 (left two columns), 6 (middle column), and 7 (right two columns). Columns labeled “COSMOS” use WMAP5+Union2+COSMOS data. Columns labeled “+CFHTLS” use WMAP5+Union2+COSMOS+CFHTLS data. Recall that in the binned parameterization, redshift bin  $a$  is  $2 < z < 9$ , redshift bin  $b$  is  $1 < z < 2$ , and redshift bin  $c$  is  $z < 1$ .

in the width of the probability distributions in Figure 5 when adding weak lensing.

The degeneracy illustrated in Figure 2 is plotted as the black, solid curve in Figure 7. The agreement with the likelihood contours is quite interesting, calling to mind the discussion in Sec. III A about parameter covariances. This arose from the observation that an unmodified Poisson equation (20) that relates the *sum* of the two metric potentials to the underlying density fluctuations leaves the large-scale CMB predictions nearly unchanged when varying the ratio of the metric potentials, i.e.  $\varpi$ . That degeneracy is due to the fact that the large-scale CMB predictions depend on the sum of the two metric potentials (cf. Eq. 19). If this sum is directly related to the underlying density perturbation then the only effect  $\varpi$  can have on the large-scale CMB is through its effect on the evolution of  $\Delta_m$ ; by contrast, if the Poisson equation is of the form of Eq. (11), where only one potential is related to  $\Delta_m$ , then  $\varpi$  also appears in a multiplicative factor. Thus the specific approaches to modifying gravity give distinct relations between the parameters and the observables.

For observations that depend on the combination  $\phi + \psi$  there will be a degeneracy along the curve (see Eqs. 13 and 15)

$$\mu = \frac{2}{2 + \varpi}. \quad (21)$$

We find numerically that this degeneracy applies approximately to both large-scale CMB as well as weak lensing observations, even though both measurements have a further dependence on  $\varpi$  and  $\mu$  through the growth factor (cf. Eq. 17). The relation in Eq. (21) gives the black, solid curve in Figure 7 and indeed is quite close to a degeneracy in the constraints.

## V. DISCUSSION

Testing general relativity on cosmological length scales is an exciting prospect enabled by improvements in data. To interpret such a test requires an approach to parameterizing modifications from GR, similar to the PPN method for tests within the solar system and using binary pulsars, but appropriate for cosmic scales. Numerous parameterizations have been suggested and we compare,

and in some cases, unify them through a “translation” table. These approaches can effectively be interpreted within one formalism with two parameters  $\varpi$  and  $\mu$  (an extension of the previous  $\varpi$ CDM scenario).

In this generalized  $\varpi\mu$ CDM model, even if the two parameters characterizing modifications to gravity are scale independent we find effects that are visible in the large-scale structure matter power spectrum, and thus in weak lensing shear correlations, that depend on scale. We give quantitative results for the effects of the modifications on the cosmic microwave background temperature power spectrum, the growth of matter density perturbations and the density power spectrum, and the weak lensing statistics, along with analysis of the physical basis of the effects. On large scales in the density power spectrum, values of  $\varpi$  or  $\mu$  above their GR values cause suppression of power while leading to enhancement on smaller scales.

We confront the modifications to GR with current cosmological observations, analyzing CMB (WMAP 5-year), supernovae (Union2), and weak lensing (CFHTLS and COSMOS) data. Employing two different forms of dependence of the modifications on redshift, we find no evidence at 95% confidence level for such extensions to GR, regardless of the combinations of data used. Note that this holds for both the data employed by [39] (which used an overspecified system of equations in that analysis), and a more comprehensive set of observations.

We also verify the trade-off between  $\varpi$  and  $\mu$  predicted analytically. Such covariance leads to an interesting degeneracy for measurements depending on the sum of the metric potentials, although growth measurements depend on a different combination. Since large scale CMB and weak lensing depend on the sum of the metric potentials, one could consider the Poisson equation for the sum, and here the key parameter is the effective Newtons constant  $\tilde{G}_{\text{eff}} = \mu(2 + \varpi)/2$ . The matter density growth factor is primarily sensitive to extensions beyond GR in terms of the factor  $\Sigma = \mu(1 + \varpi)$ . These parameters still appear to have covariance, however, in our initial explorations. Overall, this suggests that exploration of gravity through cosmological measurements requires a sufficiently flexible theory space and a diverse set of observations.

As seen from Figures 2-4, robust identification of deviations from GR will require measurement over a large range of scales. Well below the Hubble scale, the modifi-



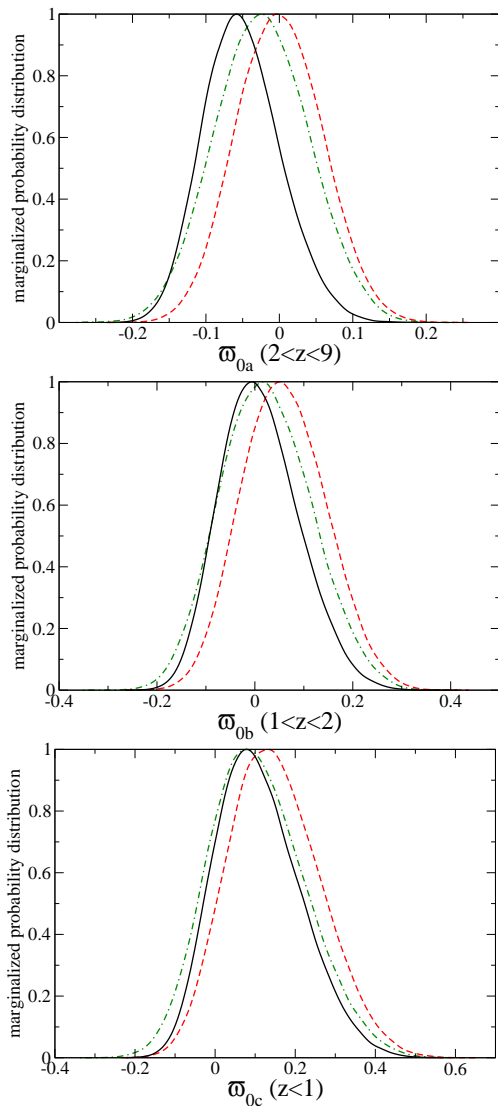


FIG. 5: Marginalized probabilities of the post-GR parameters  $\varpi_{0a,b,c}$  defined in high, medium and low redshift bins respectively. The parameter  $\mu$  has been fixed to  $\mu = 1$ , consistent with General Relativity. Green (dot-dashed) curves are constraints determined from the WMAP 5 year [57] and supernova Union2 [60] data sets only. Red (dashed) curves also include the COSMOS weak lensing tomography data [3]. Black (solid) curves use measurements of the aperture mass taken from the CFHTLS weak lensing survey [4] in addition to COSMOS, WMAP5, and Union2.

cations we have examined become scale independent and so can become confused with shifts in the fiducial amplitude ( $\sigma_8$ ), galaxy bias, or normalization errors from photometric redshift estimation of weak lensing source densities. These will need to be addressed to have confidence in claims of any detected deviation, as will allowance for expansion histories different from  $\Lambda$ CDM.

Finally, future data, including observations sensitive to growth and the growth rate, and those sensitive to the expansion history, will be essential to providing true tests

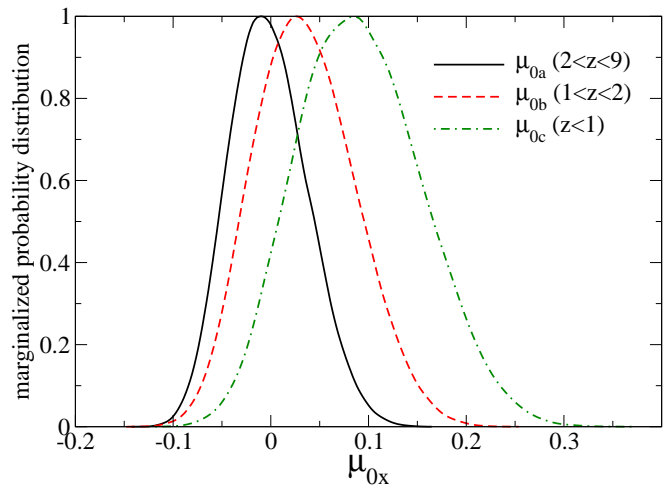


FIG. 6: Marginalized probabilities of the post-GR parameters  $\mu_{0a,b,c}$  defined in high, medium, and low redshift bins respectively. The parameter  $\varpi$  has been fixed to  $\varpi = 0$ , consistent with General Relativity. All curves show constraints derived using data from the WMAP 5 year release [57], supernova Union2 set [60], and COSMOS [3] plus CFHTLS [4] weak lensing data.

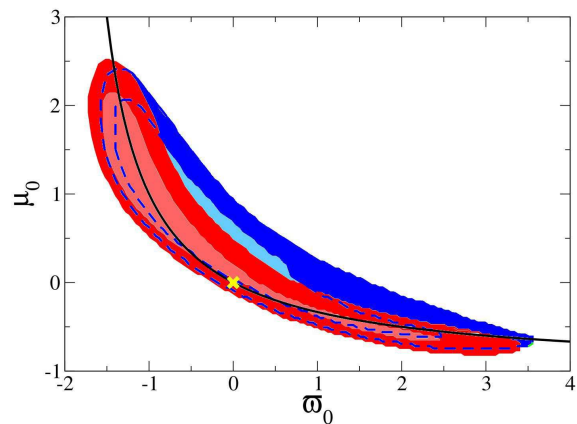


FIG. 7: 68% (inner) and 95% (outer) confidence contours for modified gravity parameters are plotted in the  $\varpi_0$ - $\mu_0$  plane (all other parameters marginalized), where  $\varpi_0$  and  $\mu_0$  are defined as in Eq. (18). Blue (background) contours use the WMAP 5 year, supernova Union2, and COSMOS data sets. Red (foreground) contours use WMAP 5 year, supernova Union2, COSMOS and CFHTLS data. The black curve plots the degeneracy direction  $\mu_0 = 2/(2 + \varpi_0) - 1$  from Figure 2. The yellow x denotes GR parameter values.

of the framework of gravity on cosmic scales.

### Acknowledgments

We are extremely grateful to the Supernova Cosmology Project for permission to use the Union2 supernova data before publication. We acknowledge the use of the Legacy Archive for Microwave Background Data Analysis (LAMBDA). Support for LAMBDA is provided by the NASA Office of Space Science. We thank Rachel Bean for helpful discussions on Ref. [39]. This work has been supported by the World Class University grant R32-2008-000-10130-0 (SD, EL). EL has been supported in part by the Director, Office of Science, Office of High Energy Physics, of the U.S. Department of Energy under Contract No. DE-AC02-05CH11231. AC acknowledges support from NSF CAREER AST-0645427. RC acknowledges support from NSF CAREER AST-0349213. LL was supported by the Swiss National Science Foundation under Contract No. 2000 124835 1.

### Appendix A: Density Perturbation Growth

We here obtain the analog of the GR second order differential equation for matter density perturbation evolution, working in the conformal Newtonian gauge. After matter-radiation decoupling, conservation of energy gives

$$\dot{\delta}_m = 3\dot{\phi} - \theta_m \quad (\text{A1})$$

$$\dot{\theta}_m = -\mathcal{H}\theta_m + k^2\psi, \quad (\text{A2})$$

assuming  $\delta p = \sigma = 0$ , i.e. there is no pressure, no pressure perturbation, and no anisotropic shear. Rearranging

Eq. (A1) and substituting Eq. (A2), we can write

$$\begin{aligned} \theta_m &= 3\dot{\phi} - \dot{\delta}_m \\ &= 3\dot{\phi} - \dot{\Delta}_m + \frac{d}{d\tau} \left( \frac{3\mathcal{H}\theta_m}{k^2} \right) \\ &= 3\dot{\phi} - \dot{\Delta}_m + \frac{3}{k^2} \left[ \theta_m \dot{\mathcal{H}} - \mathcal{H}^2\theta_m + \mathcal{H}k^2\psi \right] \\ &= \frac{3\dot{\phi} - \dot{\Delta}_m + 3\mathcal{H}\psi}{1 - 3(\dot{\mathcal{H}} - \mathcal{H}^2)/k^2}. \end{aligned} \quad (\text{A3})$$

We can use Eqs. (11) and (9) to write  $\psi$  in terms of  $\Delta_m$ ,  $\mu$ ,  $\varpi$ , and background quantities; similarly we can use the time derivative of Eq. (11) to write  $\dot{\phi}$ . This gives

$$\begin{aligned} \dot{\Delta}_m &= \dot{\delta}_m + \frac{3\dot{\mathcal{H}}\theta_m}{k^2} + \frac{3\mathcal{H}\dot{\theta}_m}{k^2} \\ &= 3\dot{\phi} - \theta_m + \frac{3\dot{\mathcal{H}}\theta_m}{k^2} + \frac{3\mathcal{H}}{k^2} (-\mathcal{H}\theta_m + k^2\psi) \end{aligned} \quad (\text{A4})$$

where the second equality comes from using Eqs. (A1) and (A2). Substituting Eq. (A3) into (A4) would just return the truism  $\dot{\Delta}_m = \dot{\Delta}_m$ . However, if we take the first conformal time derivative of Eq. (A4) before substituting, we find a second order differential equation describing the evolution of  $\Delta_m$  for arbitrary  $\varpi(a, k)$  and  $\mu(a, k)$ . We omit the explicit copious algebra and show the result:

$$\begin{aligned} \ddot{\Delta}_m \left( 1 + \frac{3}{k^2}\Gamma\mu \right) &= \dot{\Delta}_m \left\{ -\frac{3}{k^2} (2\dot{\Gamma}\mu + 2\Gamma\dot{\mu}) - \frac{3}{k^2} (1 + \varpi)\Gamma\mu\mathcal{H} + \left( \mathcal{H} + 3\frac{\ddot{\mathcal{H}}}{k^2} - 9\frac{\mathcal{H}\dot{\mathcal{H}}}{k^2} + 3\frac{\mathcal{H}^3}{k^2} \right) \times \frac{-3\Gamma\mu - k^2}{k^2 - 3(\dot{\mathcal{H}} - \mathcal{H}^2)} \right\} \\ &+ \Delta_m \left\{ -\frac{3}{k^2} (\ddot{\Gamma}\mu + \Gamma\ddot{\mu} + 2\dot{\Gamma}\dot{\mu}) - (1 + \varpi)\frac{\Gamma\mu}{k^2} (-k^2 + 6\dot{\mathcal{H}} - 3\mathcal{H}^2) - 3\dot{\varpi}\frac{\Gamma\mu}{k^2}\mathcal{H} - \frac{3}{k^2}(1 + \varpi)\mathcal{H}(\dot{\Gamma}\mu + \Gamma\dot{\mu}) \right. \\ &\left. + \left( \mathcal{H} + 3\frac{\ddot{\mathcal{H}}}{k^2} - 9\frac{\mathcal{H}\dot{\mathcal{H}}}{k^2} + 3\frac{\mathcal{H}^3}{k^2} \right) \times \frac{-3(\dot{\Gamma}\mu + \Gamma\dot{\mu}) - 3(1 + \varpi)\mathcal{H}\Gamma\mu}{k^2 - 3(\dot{\mathcal{H}} - \mathcal{H}^2)} \right\}, \end{aligned} \quad (\text{A5})$$

where  $\Gamma = 4\pi G a^2 \bar{\rho}_m$ . All that we have assumed in this derivation is that matter and  $\Lambda$  are the only constituents

of the background cosmology so that Eqs. (A1) and (A2) hold.

[1] J. Frieman, M. Turner and D. Huterer, *Ann. Rev. Astron. Astrophys.* **46**, 385 (2008) [arXiv:0803.0982 [astro-ph]].  
[2] R. R. Caldwell and M. Kamionkowski, *Ann. Rev.*

*Nucl. Part. Sci.* **59**, 397 (2009) [arXiv:0903.0866 [astro-ph.CO]].  
[3] R. Massey *et al.*, *Astrophys. J. Suppl.* **172**, 239 (2007)

- [arXiv:astro-ph/0701480].
- [4] L. Fu *et al.*, *Astron. Astrophys.* **479** 9 (2008) [arXiv:0712.0884 [astro-ph]].
- [5] E. Bertschinger, *Astrophys. J.* **648**, 797 (2006) [arXiv:astro-ph/0604485].
- [6] R. Caldwell, A. Cooray and A. Melchiorri, *Phys. Rev. D* **76**, 023507 (2007) [arXiv:astro-ph/0703375].
- [7] P. Zhang, M. Liguori, R. Bean and S. Dodelson, *Phys. Rev. Lett.* **99**, 141302 (2007) [arXiv:0704.1932 [astro-ph]].
- [8] L. Amendola, M. Kunz and D. Sapone, *JCAP* **0804**, 013 (2008) [arXiv:0704.2421 [astro-ph]].
- [9] W. Hu and I. Sawicki, *Phys. Rev. D* **76**, 104043 (2007) [arXiv:0708.1190 [astro-ph]].
- [10] M. A. Amin, R. V. Wagoner and R. D. Blandford, arXiv:0708.1793 [astro-ph].
- [11] B. Jain and P. Zhang, *Phys. Rev. D* **78**, 063503 (2008) [arXiv:0709.2375 [astro-ph]].
- [12] E. Bertschinger and P. Zukin, *Phys. Rev. D* **78**, 024015 (2008) [arXiv:0801.2431 [astro-ph]].
- [13] W. Hu, *Phys. Rev. D* **77**, 103524 (2008) [arXiv:0801.2433 [astro-ph]].
- [14] Y. S. Song and K. Koyama, *JCAP* **0901**, 048 (2009) [arXiv:0802.3897 [astro-ph]].
- [15] F. Schmidt, *Phys. Rev. D* **78**, 043002 (2008) [arXiv:0805.4812 [astro-ph]].
- [16] C. Skordis, *Phys. Rev. D* **79**, 123527 (2009) [arXiv:0806.1238 [astro-ph]].
- [17] E. V. Linder, *Phys. Rev. D* **79**, 063519 (2009) [arXiv:0901.0918 [astro-ph.CO]].
- [18] J. B. Dent, S. Dutta and L. Perivolaropoulos, *Phys. Rev. D* **80**, 023514 (2009) [arXiv:0903.5296 [astro-ph.CO]].
- [19] F. Schmidt, M. Liguori and S. Dodelson, *Phys. Rev. D* **76**, 083518 (2007) [arXiv:0706.1775 [astro-ph]].
- [20] G. B. Zhao, L. Pogosian, A. Silvestri and J. Zylberberg, *Phys. Rev. D* **79**, 083513 (2009) [arXiv:0809.3791 [astro-ph]].
- [21] L. Pogosian, A. Silvestri, K. Koyama and G. B. Zhao, arXiv:1002.2382 [astro-ph.CO].
- [22] Y. S. Song and O. Dore, *JCAP* **0903**, 025 (2009) [arXiv:0812.0002 [astro-ph]].
- [23] P. Serra, A. Cooray, S. F. Daniel, R. Caldwell and A. Melchiorri, *Phys. Rev. D* **79**, 101301 (2009) [arXiv:0901.0917 [astro-ph.CO]].
- [24] G. B. Zhao, L. Pogosian, A. Silvestri and J. Zylberberg, *Phys. Rev. Lett.* **103**, 241301 (2009) [arXiv:0905.1326 [astro-ph.CO]].
- [25] J. Guzik, B. Jain and M. Takada, *Phys. Rev. D* **81**, 023503 (2010) [arXiv:0906.2221 [astro-ph.CO]].
- [26] A. Kosowsky and S. Bhattacharya, *Phys. Rev. D* **80**, 062003 (2009) [arXiv:0907.4202 [astro-ph.CO]].
- [27] E. Beynon, D. J. Bacon and K. Koyama, *Mon. Not. Roy. Astron. Soc.* **403**, 353 (2010) arXiv:0910.1480 [astro-ph.CO].
- [28] K. W. Masui, F. Schmidt, U. L. Pen and P. McDonald, *Phys. Rev. D* **81**, 062001 (2010) arXiv:0911.3552 [astro-ph.CO].
- [29] Y. S. Song, L. Hollenstein, G. Caldera-Cabral and K. Koyama, arXiv:1001.0969 [astro-ph.CO].
- [30] W. Cui, P. Zhang and X. Yang, arXiv:1001.5184 [astro-ph.CO].
- [31] C. Di Porto and L. Amendola, *Phys. Rev. D* **77**, 083508 (2008) [arXiv:0707.2686 [astro-ph]].
- [32] S. Nesseris and L. Perivolaropoulos, *Phys. Rev. D* **77**, 023504 (2008) [arXiv:0710.1092 [astro-ph]].
- [33] O. Dore *et al.*, arXiv:0712.1599 [astro-ph].
- [34] S. F. Daniel, R. R. Caldwell, A. Cooray and A. Melchiorri, *Phys. Rev. D* **77**, 103513 (2008) [arXiv:0802.1068 [astro-ph]].
- [35] R. E. Smith *et al.* [The Virgo Consortium Collaboration], *Mon. Not. Roy. Astron. Soc.* **341**, 1311 (2003) [arXiv:astro-ph/0207664].
- [36] K. Yamamoto, T. Sato and G. Huetsi, *Prog. Theor. Phys.* **120**, 609 (2008) [arXiv:0805.4789 [astro-ph]].
- [37] S. F. Daniel, R. R. Caldwell, A. Cooray, P. Serra, A. Melchiorri, *Phys. Rev. D* **80**, 023532 (2009) [arXiv:0901.0919 [astro-ph.CO]].
- [38] T. Giannantonio, M. Martinelli, A. Silvestri and A. Melchiorri, arXiv:0909.2045 [astro-ph.CO].
- [39] R. Bean, arXiv:0909.3853 [astro-ph.CO].
- [40] B. Bertotti, L. Iess and P. Tortora, *Nature* **425**, 374 (2003).
- [41] S. S. Shapiro, J. L. Davis, D. E. Lebach and J. S. Gregory, *Phys. Rev. Lett.* **92**, 121101 (2004).
- [42] J. H. Taylor, *Rev. Mod. Phys.* **66**, 711 (1994).
- [43] A. G. Lyne *et al.*, *Science* **303**, 1153 (2004) [arXiv:astro-ph/0401086].
- [44] C. M. Will, "Theory and experiment in gravitational physics," *Cambridge, UK: Univ. Pr. (1993) 380 p*
- [45] C. M. Will, *Living Rev. Rel.* **9**, 3 (2006) [arXiv:gr-qc/0510072].
- [46] C. P. Ma and E. Bertschinger, *Astrophys. J.* **455**, 7 (1995) [arXiv:astro-ph/9506072].
- [47] M. S. Turner and A. G. Riess, *Astrophys. J.* **569**, 18 (2002) [arXiv:astro-ph/0106051].
- [48] E. V. Linder, *Phys. Rev. D* **72**, 043529 (2005) [arXiv:astro-ph/0507263].
- [49] E. V. Linder and R. N. Cahn, *Astropart. Phys.* **28**, 481 (2007) [arXiv:astro-ph/0701317].
- [50] P. Zhang, *Astrophys. J.* **647**, 55 (2006) [arXiv:astro-ph/0512422].
- [51] U. Seljak and M. Zaldarriaga, *Astrophys. J.* **469**, 437 (1996) [arXiv:astro-ph/9603033].
- [52] A. Lewis, A. Challinor and A. Lasenby, *Astrophys. J.* **538**, 473 (2000) [arXiv:astro-ph/9911177].
- [53] [http://lambda.gsfc.nasa.gov/product/map/dr3/params/lcdm\\_sz\\_lens\\_wmap5.cfm](http://lambda.gsfc.nasa.gov/product/map/dr3/params/lcdm_sz_lens_wmap5.cfm)
- [54] A. Lewis and S. Bridle, *Phys. Rev. D* **66**, 103511 (2002) [arXiv:astro-ph/0205436].
- [55] A. Lewis and S. Bridle, <http://cosmologist.info/notes/COSMOMC.ps.gz>
- [56] J. Lesgourgues, M. Viel, M. G. Haehnelt and R. Massey, *JCAP* **0711**, 008 (2007) [arXiv:0705.0533 [astro-ph]].
- [57] J. Dunkley *et al.* [WMAP Collaboration], *Astrophys. J. Suppl.* **180**, 306 (2009) arXiv:0803.0586 [astro-ph].
- [58] M. R.olta *et al.* [WMAP Collaboration], *Astrophys. J. Suppl.* **180**, 296 (2009) [arXiv:0803.0593 [astro-ph]].
- [59] G. Hinshaw *et al.* [WMAP Collaboration], *Astrophys. J. Suppl.* **180**, 225 (2009) [arXiv:0803.0732 [astro-ph]].
- [60] R. Amanullah *et al.*, *Astrophys. J.* **716**, 712 (2010) [arXiv:1004.1711 [astro-ph.CO]].